Dual-View and Multi-Content Head-Up Display Using a Single Picture Generation Unit and Two-Layer Volume Holographic Grating

Zhenlv Lv, Juan Liu, and Yan Yang

***Abstract*—Considering that the driver and passengers need different display content in the vehicle display, we propose a dual-view and multi-content head-up display (HUD). Based on the angle selectivity of volume holographic grating (VHG), the multiplexed VHGs diffract light beams at different angles to achieve dual-view display. Based on the wavelength selectivity of VHG, the multiplexed VHGs diffract light beams of different wavelengths that carry different information to realize multi-content display. The HUD prototype is composed of a miniature laser projector, a diffuser, and a holographic combiner. The holographic combiner with a size of 20 cm × 15 cm includes a red-green multiplexed VHG_1, a red-blue multiplexed VHG_2 and a glass substrate. The field of views (FOVs) and eye-boxs (EBs) of the two viewing zones are 10° × 5° and 8° × 4°, 147 mm × 81 mm and 105 mm × 87 mm, respectively. In addition, compared with the traditional dual-view HUD, the proposed HUD only requires one picture generation unit (PGU), which is beneficial for its application to compact vehicle or aviation displays. Moreover, the driver and passengers can see the red warning information displayed by the system at the same time, which can significantly improve driving safety.**

***Index Terms*—Holography, diffractive imaging, imaging systems.**

I. Introduction

THE head-up display (HUD) is a navigation device that projects important driving information such as speed and navigation to the outside of the windshield through a combiner [1], [2]. The driver can see all driving information through the HUD, without having to look down at the dashboard. Because it can significantly improve driving safety, HUD has been widely used in aviation, automobiles, and motorcycles [3].

HUDs on the market include windshield-HUD (W-HUD), combiner-HUD (C-HUD) and augmented reality-HUD (AR-HUD) [4]–[6]. In recent years, AR HUD has been constantly mentioned and discussed as an upgraded version of W-HUD. With a larger field of view (FOV), longer imaging distance, and higher dynamic range, combined with sensing technology and communication technology, AR HUD can provide drivers with a better driving experience combining virtual and real [7], [8].

In addition to large FOV and long imaging distance, another actual need of AR HUD is to provide driver and passenger with their respective required display content, such as providing navigation information for the driver and entertainment information for the passenger. Therefore, the HUD needs to be designed to achieve dual-view display. Many researches have been done on the design of dual-view display on liquid crystal displays and integrated imaging three-dimensional displays [9]–[14]. However, there are relatively few studies on dual-view HUD. The typical method to realize dual-view HUD is to assemble two sets of HUDs corresponding to the driver and passenger respectively [15], as shown in Fig. 1(a). But this method will make the system huge and cannot be integrated in the limited space below the dashboard. Yutaka Tokuda *et al.* proposed dual-view display through a half mirror and two displays covered by a transparent retro-reflector [16]. In addition to the large system volume, this method also has the problems of short imaging distance and image crosstalk in different viewing angles. Chun-Yao Shih *et al.* proposed a binocular eye-box (EB) HUD with a wider display range through a specially designed laminate combiner [17]. The dual-view range of this method is limited because it only expands the observation area of a driver. In addition, since only one display is used as the image source, it is impossible to provide different display contents for the driver and passenger.

The above-mentioned dual-view HUD methods are all based on geometric optical elements. Volume holographic gratings (VHGs) have excellent wavelength and angle selectivity and have been widely used in thin and light AR head-mounted displays and head-up displays [18]–[23]. VHGs with excellent angle selectivity are very suitable for multi-view display through multiplexing or layering [24], [25]. In addition, the excellent wavelength selectivity of VHGs enables HUD to provide the same or different display content for different viewing angles with only one image source, thereby reducing the system volume.

In this paper, we propose a VHG-based dual-view and multi-content HUD system with only one picture generation unit (PGU), as shown in Fig. 1(b). Based on the angle selectivity

Manuscript received April 11, 2022; revised May 23, 2022; accepted June 6, 2022. Date of publication June 10, 2022; date of current version June 17, 2022. This work was supported in part by National Natural Science Foundation of China under Grants 61975014 and 62035003 and in part by Beijing Municipal Science and Technology Commission, Administrative Commission of Zhongguancun Science Park under Grant Z211100004821012. *(Corresponding author: Juan Liu.)*

The authors are with the Beijing Engineering Research Center for Mixed Reality and Advanced Display, School of Optics and Photonics, Beijing Institute of Technology, Beijing 100081, China (e-mail: 3120195305@bit.edu.cn; juanliu@bit.edu.cn; 13693674145@163.com).

This article has supplementary downloadable material available at https://doi.org/10.1109/JPHOT.2022.3181620, provided by the authors.

Digital Object Identifier 10.1109/JPHOT.2022.3181620

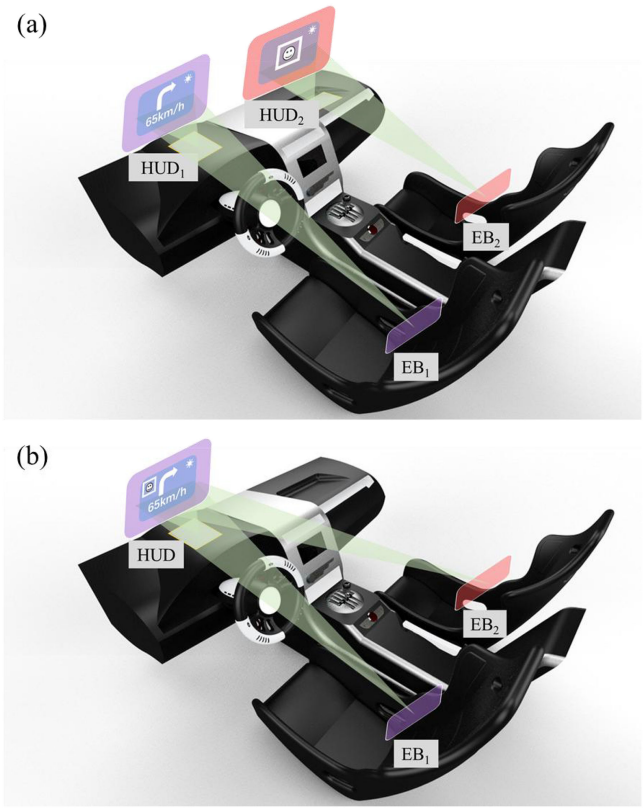

Fig. 1. (a) Traditional dual-view HUD system. (b) The dual-view and multi-content HUD system proposed in this paper. The traditional method requires two sets of HUDs, which is bulky and expensive. Our proposed method using VHG requires only one HUD to achieve dual viewing angle display, and the images viewed at different viewing angles can be either the same or different due to the wavelength selectivity of VHG.

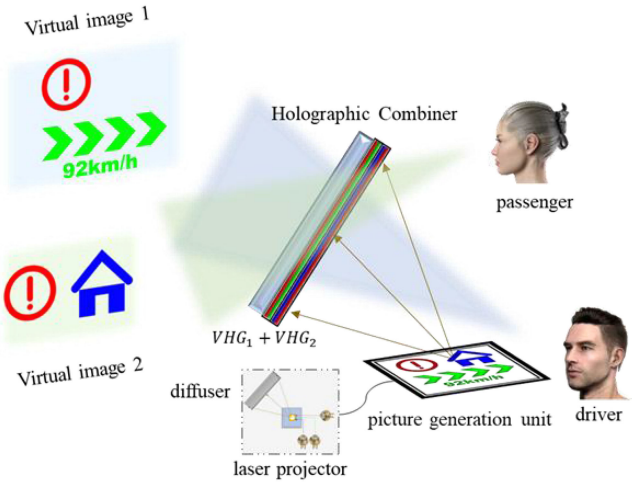

Fig. 2. Schematic diagram of the proposed multi-view and multi-content holographic head-up display system.

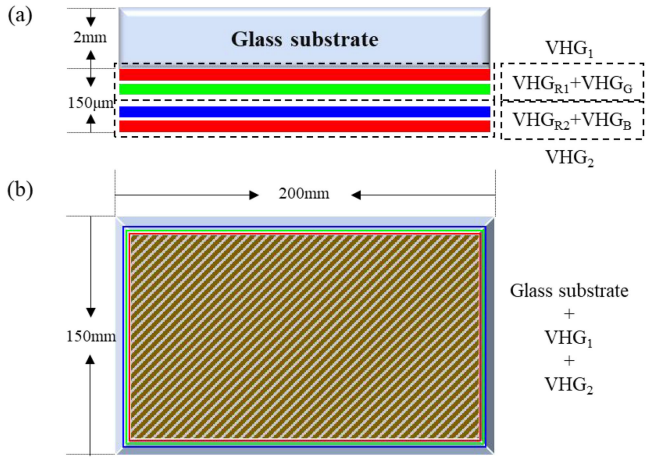

Fig. 3. (a) and (b) are the structure and size parameters of the holographic combiner.

of VHGs, layered VHGs can diffract light beams of different wavelengths at different angles to achieve dual-view display. Based on the wavelength selectivity of VHGs, the display content provided by the HUD system for the driver and passenger can be the same display content of the same wavelength or different content of different wavelengths.

II. System Design

A. Structure and Principle

The structure diagram of the system composed of PGU and holographic combiner is shown in Fig. 2. The PGU including a miniature laser projector and a diffuser is used to generate and project the target image corresponding to the dual viewing angle to the holographic combiner. As the core imaging element of the system, the holographic combiner composed of a glass substrate, a red-green wavelength-multiplexed VHG_1 corresponding to viewing angle 1, and a red-blue wavelength-multiplexed VHG_2 corresponding to viewing angle 2, has the functions of image magnification and dual viewing angle deflection.

VHG_1 and VHG_2 have the same incident angles from the image source but different diffraction angles corresponding to driver and passenger respectively. In detail, because VHG_1 and VHG_2 have angular selectivity and wavelength selectivity corresponding to blue and green, dual-view and multi-content display can be realized with only one image source that loads green and blue images. In addition, because VHG_1 and VHG_2 also contain holographic gratings sensitive to red light waves, the system can realize information sharing between driver and passenger. For example, navigation information is only presented to the driver through green light, entertainment information is only presented to passengers through blue light, and vehicle warning information is presented to the driver and passengers at the same time through red light. Additionally, lens-enabled VHGs avoid adding extra lenses to the projection module, making the system lighter and smaller.

The core of the HUD system is the holographic combiner. The structure and size parameters of the holographic combiner are shown in the Fig. 3. Fig. 3(a) and (b) are side and top views of the holographic combiner. The holographic combiner is composed of a glass substrate and VHGs. VHGs are composed of VHG_1 and VHG_2 by vacuum bonding. VHG_1 includes VHG_{R1} which is sensitive to red light and VHG_G which is sensitive to green

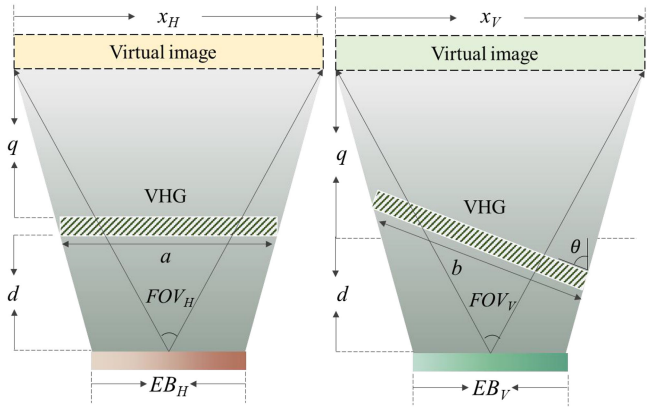

Fig. 4. Schematic diagram of FOV and EB in horizontal and vertical directions.

light. VHG_2 includes VHG_{R2} which is sensitive to red light and VHG_B which is sensitive to blue light. It is important to point out that although both VHG_{R1} and VHG_{R2} are sensitive to red light, they have different diffraction angles. Moreover, the thickness of the glass substrate and VHGs are 2 mm and 150μm, respectively. In addition, the size of the holographic combiner is 200 mm $\times$ 150 mm.

B. FOV and EB

The HUD system proposed in this paper provides independent green and blue information and shared red signals to the driver and passenger at the same time, so it can ensure the privacy of the driver and passenger and improve driving safety. Considering the safety of the car when driving on the actual road, there is another urgent requirement that the driver should avoid viewing the entertainment information provided to the co-driver. Therefore, when designing the system parameters, it should be noted that the eye-box of driver and passenger cannot overlap. When the size of the object surface is small, each pixel can be diffracted by VHGs, and the FOV and eye-box of the HUD can be analyzed by geometric relationship without considering the angular selectivity of VHGs.

The schematic diagrams of FOV and EB in the horizontal and vertical directions are shown in Fig. 4. q is the distance of the virtual image formed by the VHGs. d is the distance between the observer and the VHGs. x_H and x_V are the horizontal and vertical sizes of the virtual image displayed by the system. x_{H0} and x_{V0} are the horizontal and vertical sizes of the original image loaded on the image source. p is the distance between the image source and the VHGs.

The FOV of the system can be expressed as:

$$FOV_H = 2\arctan\left[\frac{x_H}{2\,(q+d)}\right] = 2\arctan\left[\frac{qx_{H0}}{2p\,(q+d)}\right] \tag{1}$$

$$FOV_V = 2\arctan\left[\frac{x_V}{2\,(q+d)}\right] = 2\arctan\left[\frac{qx_{V0}}{2p\,(q+d)}\right] \tag{2}$$

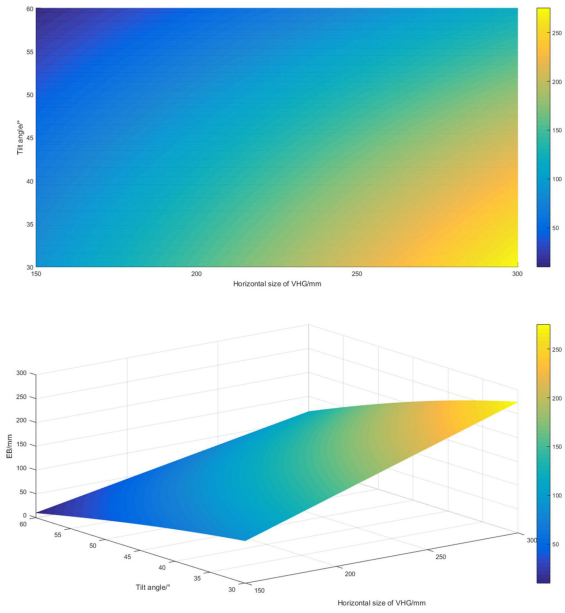

Fig. 5. Relationship between the inclination angle, the horizontal size of the VHGs, and the passenger's horizontal EB.

The EB of the system can be expressed as:

$$\begin{aligned} EB_H &= a\cos\varphi - (x_H - a\cos\varphi)\,\frac{d}{q} \\ &= a\cos\varphi - \left(\frac{qx_{H0}}{p} - a\cos\varphi\right)\frac{d}{q} \end{aligned} \tag{3}$$

$$\begin{aligned} EB_V &= b\sin\theta - (x_V - b\sin\theta)\,\frac{d}{q} \\ &= b\sin\theta - \left(\frac{qx_{V0}}{p} - b\sin\theta\right)\frac{d}{q} \end{aligned} \tag{4}$$

Where a and b are the horizontal and vertical sizes of the VHGs. φ is the tilt angle in the horizontal direction when viewing, and this value is 0 for the front viewing angle. And θ is the inclination angle of the VHGs in the vertical direction.

For the driver in front of the HUD, there is no loss of EB in the horizontal direction, and EB in the vertical direction is lost due to inclination. For the passenger on the side of the HUD, both the horizontal and vertical EB are lost due to the inclination. And the inclination angle will directly affect the EB of the passenger in the horizontal direction. Therefore, we analyzed the relationship between inclination angle, VHGs size and horizontal EB, as shown in Fig. 5. If the horizontal size of VHGs is fixed, the inclination angle is negatively correlated with the horizontal EB. For example, when the horizontal size of the VHGs is 200 mm and the inclination angle is increased to 55°, the horizontal EB will be reduced to 67 mm. In order to achieve a large horizontal EB with a large inclination angle, the horizontal size of the VHGs should be increased.

Based on the above formulas and theoretical derivation, after weighing the various parameters of HUD, the detailed parameters of VHG_1 and VHG_2 are listed in Table I.

TABLE I
THE DESIGN PARAMETERS OF HOE_R, HOE_G AND HOE_B

Parameters	VHG_1 (VHG_{R1}+VHG_G)	VHG_2 (VHG_{R2}+VHG_B)
d (mm)	460	650
p (mm)	250	250
q (mm)	2000	1500
f (mm)	285.7	300
θ	45°	45°
φ	0	45°
FOV	10°×5°	6°×4°
EB (mm×mm)	147×81	105×87
Original image size (mm×mm)	53.8×26.9	37.5×25.0

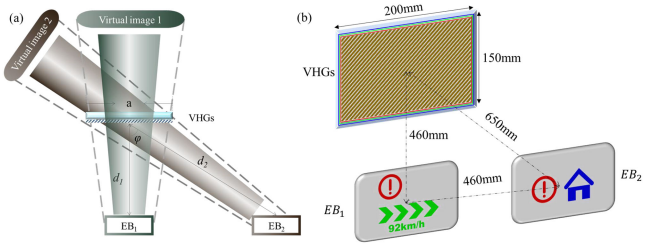

Fig. 6. (a) and (b) are the structure and size parameters of the holographic combiner.

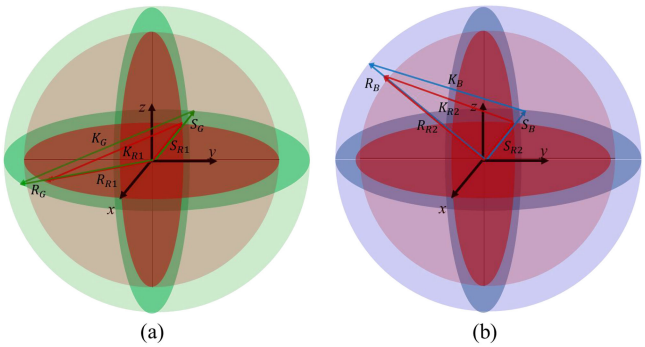

Fig. 7. (a) and (b) are K-vector diagrams of the reflection VHG_1 and VHG_2.

It can be seen from the parameters listed in the above table that the distance between driver and passenger is 460 mm, the EB of driver is 147 mm × 81 mm, and the EB of passenger is 105 mm × 87 mm. Therefore, there is no overlap between the EBs of different observers, as shown in the Fig. 6.

C. VHG_1 and VHG_2

It can be known from the coupled wave theory that the incident light vector, diffracted light vector, and grating vector form an isosceles triangle in the vector circle. When the Bragg condition is satisfied, the direction of the diffracted light during reconstruction is consistent with the direction of object light during recording, and the diffraction efficiency is the highest. The vector circles of VHG_1 and VHG_2 are shown in the Fig. 7. The vector diagrams of VHG_{R1} and VHG_G in VHG_1 are shown by the red and green lines in Fig. 7(a). It can be seen from the figure that $VHGR_1$ and VHG_G have the same grating stripe arrangement direction because the recording angle is the same. Due to the different recording wavelengths, the periods of the two gratings are different. In addition, the triangle formed by the incident light vector, the diffracted light vector, and the grating vector is located in the x-y plane. The vector diagrams of VHG_{R2} and VHG_B in VHG_2 are shown by the red and blue lines in Fig. 7(b). Different from VHG_1, the vector triangles of the two gratings in VHG_2 are located in the x-y-z three-dimensional vector sphere. The grating stripes of VHG_{R2} and VHG_B have the same arrangement direction and different periods.

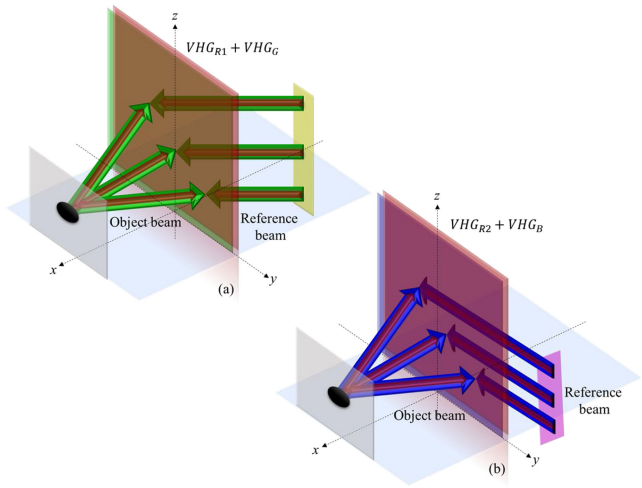

Fig. 8. (a) The recording principle of VHG_{R1} and VHG_G in VHG_1. (b) The recording principle of VHG_{R2} and VHG_B in VHG_2.

The VHG_1 used to provide the target image for driver is composed of VHG_{R1} and VHG_G. The VHG_2 used to provide the target image for passenger consists of VHG_{R2} and VHG_B. The recording methods of VHG_1 and VHG_2 are shown in Fig. 8(a) and (b). Both VHG_1 and VHG_2 are formed by the interference of a spherical object light wave perpendicular to the holographic recording plane and a plane reference light inclined to the holographic recording plane. And the holographic recording material is located in the y-z plane. However, the angle between the reference light and the holographic recording plane is different for VHG_1 and VHG_2. For VHG_1, the reference light is parallel to the x-y plane and forms an angle of 45° with the x-z plane. For VHG_2, the reference light forms an angle of 45° with the x-y plane and the x-z plane. The crosstalk between the reflection images of the glass substrate and the diffraction images of the VHGs can be avoided because the reference beams of VHG_1 and VHG_2 have an inclination angle of 45° with the x-z plane. Driver and Passenger can see the target images from different angles because the reference light of VHG_1 is parallel to the x-y plane but the reference light of VHG_2 forms an angle of 45° with the x-y plane. In addition, since the red-sensitive VHGs in VHG_1 and VHG_2 have the same recording wavelength and different recording angles, the same red image can be presented to driver and passenger at different angles.

TABLE II
THEORETICAL CALCULATION OF THE LOSS OF DIFFRACTION EFFICIENCY DUE TO WAVELENGTH SHIFT

Recording wavelength	Reconstruction wavelength	Wavelength offset	Efficiency loss
639nm	636nm	3nm	1.02%
532nm	528nm	4nm	2.31%
457nm	452nm	5nm	14.57%

III. EXPERIMENTAL VERIFICATION

A. *Diffraction Efficiency and Uniformity*

Energy utilization and display uniformity are the focus of HUD research. Therefore, we analyze and discuss the diffraction efficiency and uniformity in the dual-view HUD.

First, the wavelength of the laser projector used in the HUD prototype is inconsistent with the wavelength of the holographic exposure, resulting in not satisfying the Bragg condition, so the diffraction efficiency will be lost. We calculated the loss of diffraction efficiency due to wavelength shift based on Kogelnik's coupled-wave theory [26]. When wavelength λ beams are incident on the VHG recorded with wavelength λ_0 at the original reference beam angle, a Bragg mismatch parameter will be introduced as follows:

$$\xi = \frac{d}{2\cos\theta_s}\left(K\cos(\phi-\theta_r) - \frac{K^2\lambda}{4\pi n}\right) \tag{5}$$

where $K = 2\pi n/\lambda_0$ is the grating vector, λ_0 is the recording wavelength, d is the grating thickness, θ_s is the diffraction angle, n is the bulk index of refraction of the material, θ_r is the incident angle of reconstruction wave, φ is the tilt angle of grating vector, and λ is the wavelength of reconstruction wave. Set d and n to be 15 μm and 1.5. And the refractive index modulation is 0.03. The recording wavelengths are 639 nm, 532 nm, and 457 nm, and the output wavelengths of the laser projector are 637 nm, 528 nm, and 452 nm. We can calculate the diffraction efficiency loss due to wavelength shift, as listed in Table II. Theoretical calculations show that blue has the most efficiency loss compared to red and green. Based on the coupled wave theory, the effects of wavelength shift and material shrinkage can be improved by precompensating the recording angle, which means that the Bragg condition is still satisfied when the reconstructed wavelength is inconsistent with the recording wavelength, thereby reducing the loss of diffraction efficiency [27]. In addition, the holographic multiplexing of the grating in this paper will further lead to the reduction of diffraction efficiency. Therefore, in order to achieve uniform brightness of RGB, we adjusted the recording dosage of red, green and blue during the recording process of VHG_1 and VHG_2, increasing blue and decreasing green and red appropriately.

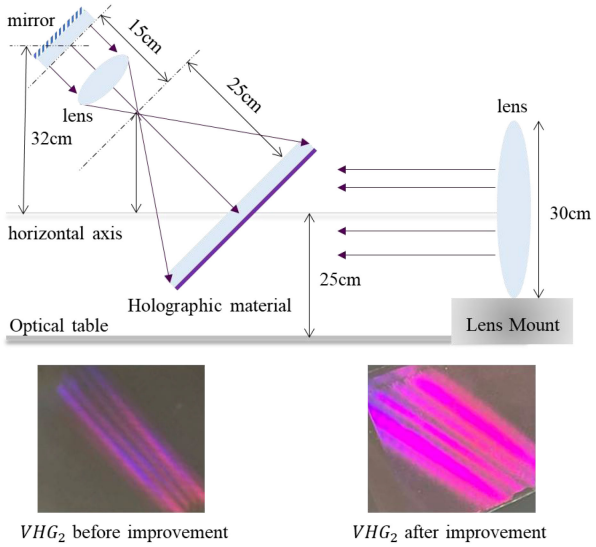

Fig. 9. Holographic exposure system.

TABLE III
COMPARISON OF DIFFRACTION EFFICIENCY OF VHGS BEFORE AND AFTER IMPROVEMENT

	VHG_1		VHG_2	
	VHG_R	VHG_G	VHG_R	VHG_B
Before improvement	35%	40%	11%	7%
After improvement	25%	23%	21%	24%

Second, interference-recorded holographic gratings also suffer from efficiency losses due to environmental instability, especially for large-sized gratings. The recording beam of the VHG_2 is tilted 45° both horizontally and vertically. One of the parallel beams and spherical beams must be incident obliquely from above. If the parallel beam from the lens with a diameter of 30 cm and the large-sized mirror is incident from a high angle obliquely above, the stability of the optical table will be extremely demanding. The experimental results show that the diffraction efficiency of VHG_2 is much lower than that of VGH_1. Considering that the spherical beam is from a 5 mm diameter achromatic lens and a small size mirror, the small optics are easy to fix. Therefore, in the experiment, we changed to the method that the holographic material is tilted and fixed, the parallel beam is parallel to the optical table, and the spherical beam is incident from obliquely above, as shown in Fig. 9. The diffraction efficiency of VHG_2 is increased to 2.5 times by the improved method. The display uniformity of the HUD proposed in this paper includes the image brightness of two viewing angles and the brightness of two colors in each viewing angle. VHG_1 needs to sacrifice some efficiency to match VHG_2. By adjusting the recording dosage of RGB and improving the stability of the exposure system, the uniformity of the diffraction efficiency of the dual-view HUD has been significantly improved, as shown in Table III. The diffraction efficiency in the Table III is measured

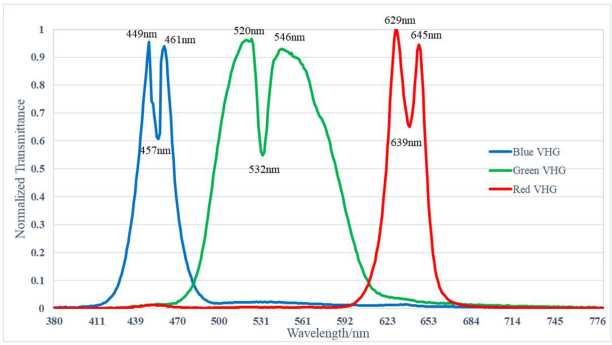

Fig. 10. Wavelength-selective properties of VHGs.

by calculating the ratio of the diffracted light energy to the incident light energy.

In addition, we experimentally evaluate the image uniformity across the FOV by partitioning the diffraction image with 8 horizontal regions and 3 vertical regions [28]. The measurement results show that the average uniformity of red and green in VHG_1 is 70% and 72%, and the average uniformity of red and blue in VHG_2 is 66% and 69%.

We further tested the wavelength-selective properties of VHGs by using a broadband LED light source, as shown in Fig. 10, where the horizontal axis is wavelength and the vertical axis is normalized transmittance. For the broadband light source, the peak diffraction wavelength of VHGs is consistent with the recording wavelength, but the broadband light source will introduce serious aberrations as the image source. Therefore, the image source in the display experiment is still a laser projector.

B. Dual-View and Multi-Content Display

Based on the theoretically designed parameters, VHGs corresponding to different viewing angles are recorded through holographic interference exposure. VHG_1 and VHG_2 are volume holographic gratings of red-green multiplexing and red-blue multiplexing, respectively. Moreover, VHG_1 and VHG_2 both use a process of simultaneous exposure at different wavelengths. The red, green and blue lasers used for exposure are high-power single-longitudinal-mode lasers. And the holographic recording material is Bayfol HX200. For VHG_1, red and green with an intensity ratio of 1:1.5 were exposed simultaneously for a total exposure of 20mJ/cm^2. For VHG_2, red and blue with an intensity ratio of 1:2 were exposed simultaneously for a total exposure of 25mJ/cm^2.

The feasibility of the method proposed in this paper is verified by incident the red, green and blue reference lights into the manufactured VHG_1 and VHG_2. We performed diffraction reconstruction on the original optical paths of VHG_1 and VHG_2 on different glass substrates to illustrate the dual-view and multi-wavelength display functions of the system. First, the three reference beams of red, green and blue are incident perpendicularly to VHG_1 composed of VHG_{R1} and VHG_G. Only the red and green light beams are diffracted obliquely to the observation plane 1, and the blue light is not modulated, as shown in Fig. 11(a). Then, the three reference beams of red, green and blue are incident on the VHG_2 composed of the VHG_{R2} and

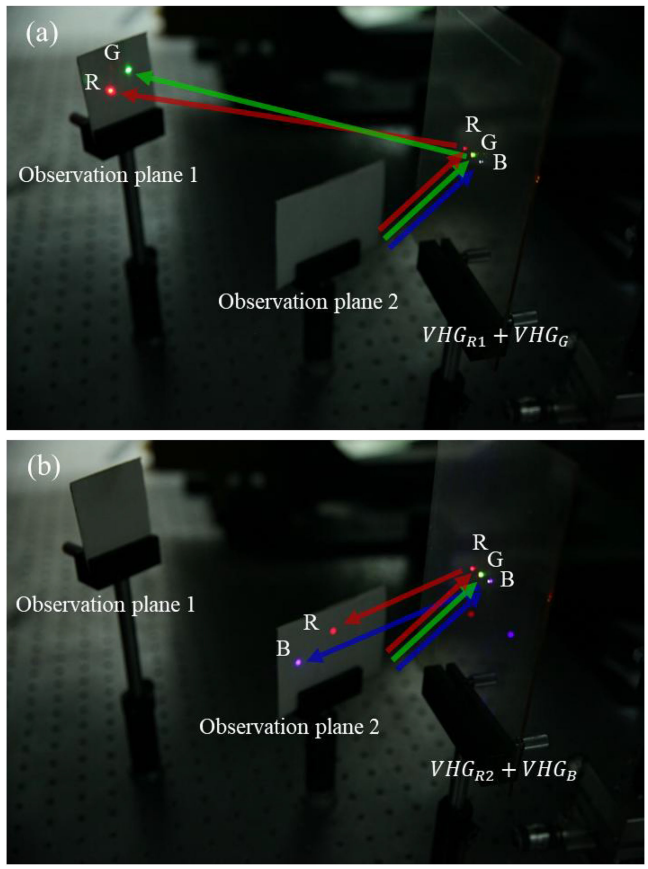

Fig. 11. (a) The diffraction effect of VHG_1 on the red, green and blue laser beams. (b) The diffraction effect of VHG_2 on the red, green and blue laser beams.

VHG_B at the same angle. Different from the diffraction effect of VHG_1, only the red and blue light beams are obliquely diffracted by VHG_2 to the observation plane 2, and the red light is not modulated, as shown in Fig. 11(b).

The prototype of the dual-view HUD system includes three parts: a laser projector, a diffuser screen and a holographic combiner, as shown in the Fig. 12. The light source is a miniature laser projector manufactured by Ultimems with a brightness of 30 lumens, a horizontal divergence angle of 43.15°, and a resolution of 1280 × 760. The diffuser is Thorlabs' DG100 × 100–1500 with a size of 100 m × 100 mm. The holographic combiner consists of a glass substrate and two layers of VHGs. To achieve high brightness and high transmittance, a vacuum bonding method is used to stack red-green wavelength-multiplexed and red-blue wavelength-multiplexed VHGs on the same glass substrate with a thickness of 2 mm. The size of the manufactured VHGs is 20 cm × 15 cm. The position of the laser projector and the diffuser in the prototype is fixed, but the distance between the holographic combiner and the diffuser is adjustable. In the actual use of the prototype, the object distance can be flexibly changed to achieve AR display with different magnifications and different depths. When the object distance is 250 mm, the display parameters of the system are consistent with the theoretical design.

The multi-view and multi-content display effects of the system have been verified by experiments, as shown in Visualization 1. The image source loads the target signal of

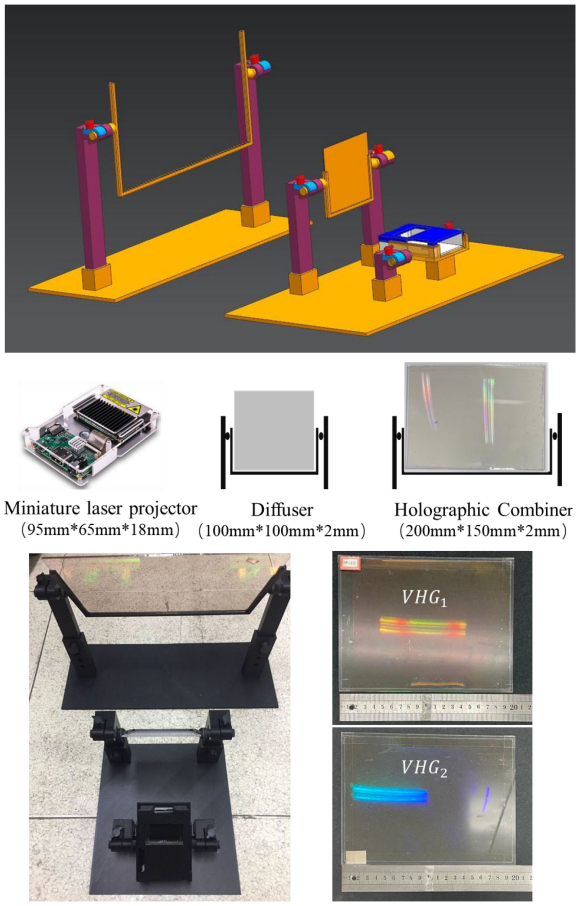

Fig. 12. The prototype of the HUD system.

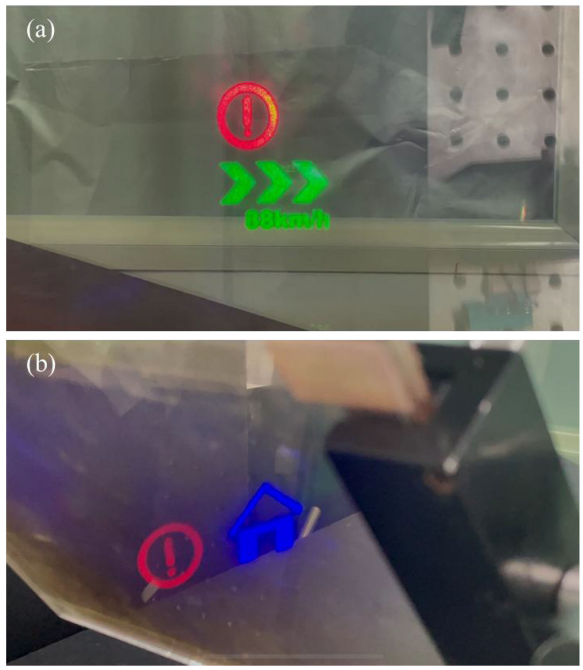

Fig. 13. The dual-view and multi-content display effect of the HUD (see Visualization 1). (a) front view. (b) oblique view.

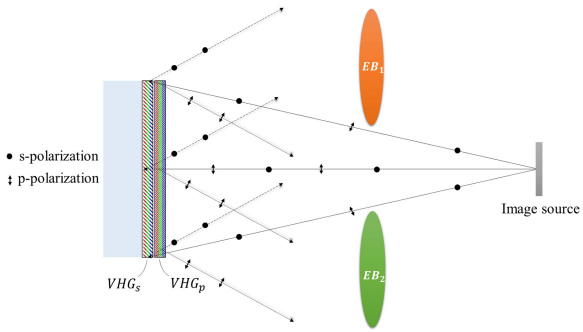

Fig. 14. Schematic diagram of the color display of the dual-view HUD proposed in this paper based on polarized VHG.

three colors of red, green and blue at the same time. The green image is navigation information only provided to the driver. And the blue image is entertainment information only provided to the passenger. Moreover, the red image is the road condition warning information provided to the driver and the passenger at the same time. Therefore, driver can see the green navigation information and the red warning signal as shown in Fig. 13(a), and passenger can see the blue entertainment information and the red warning signal as shown in Fig. 13(b). In other words, the HUD system can provide both shared information and private information to driver and passenger at the same time. Since the VHGs in the system are recorded off-axis and are not corrected for aberrations, the system suffers from vertical astigmatism, horizontal coma, and defocusing, and the aberrations increase as the angle of incidence deviates from the Bragg matching angle. Therefore, in order to improve the imaging quality of the HUD system, the VHGs should meet the Bragg matching condition during reconstruction. To further correct aberrations, a compensating cylindrical lens can be added to the recording optical path, or the exposure method can be changed to wavefront printing with high flexibility and degrees of freedom [29], [30].

The transmittance of ambient light is one of the important parameters of the HUD, so we further measured the overall transmittance of the prototype. The transmittance of the two-layer holographic film and the transmittance of the glass substrate were measured by a transmittance meter LS116 to be 77% and 90%, respectively. Moreover, the holographic combiner in the prototype including two layers of holographic film and glass substrate has a transmittance of about 70% to visible light. In addition, the selection of substrates with higher transmittance can further improve the transmittance of the system.

The display information in the dual-view and multi-content HUD proposed in this paper is related to the wavelength, green is only for the driver, and blue is only for the passenger, which means that the passenger and driver still see a monochrome image. Considering the importance of full color display, we look forward to the possibility of further realizing color display based on this work in the future. It is not feasible to directly record ordinary color VHGs with two different angles of selectivity, because the crosstalk between the images from the two viewing angles of the driver and passenger cannot be avoided. A feasible method is to use polarized VHGs as diffractive elements. The image source is used to generate two color images with different polarizations simultaneously, and the holographic combiner includes color VHG_s and VHG_p with different polarization

selectivity and different angle selectivity, as shown in Fig. 14. Color VHGs can be obtained by multiplexing or layering, and the multiplexing method should be preferred in consideration of light transmittance. This method can avoid the crosstalk of images from different angles while realizing dual-view color display.

IV. Conclusion

We propose a dual-view and multi-content HUD system based on volume holographic gratings. Based on the angle selectivity of VHG, multiplexed VHGs diffracted beams from different angles to realize dual-view display. Based on the wavelength selectivity of VHG, multiplexed VHGs diffracted beams of different wavelengths carrying different information to realize multi-content display. The display content provided by the HUD for the driver and passenger can be the same display content of the same wavelength, or different content of different wavelengths. The HUD prototype is composed of a miniature laser projector, a diffuser, and a multiplexed holographic combiner. The holographic combiner with a size of 20 cm $\times$ 15 cm includes a red-green multiplexed VHG_1, a red-blue multiplexed VHG_2 and a glass substrate. The FOVs of the driver and passenger in the dual-view HUD are 10° $\times$ 5° and 8° $\times$ 4°. And the EBs of the driver and passenger are 147 mm $\times$ 81 mm and 105 mm $\times$ 87 mm. For the HUD proposed in this paper, the driver and passenger can view their respective contents diffracted by green VHG and blue VHG from different viewing angles, and can also view the same warning signal diffracted by red VHG at the same time. This means that the driver and passenger can alert each other about road conditions while viewing their respective images through the HUD. In addition, the red, green and blue target images are provided by a PGU, which makes the system very integrated. Therefore, the proposed HUD system can be applied to in-vehicle or aviation displays in the future due to its advantages in terms of safety and compactness.

Acknowledgment

The authors would like to thank the anonymous reviewers for their valuable suggestions.

References

[1] M. O. Freeman, "MEMS scanned laser head-up display," in *Proc. MOEMS Miniaturized Syst. X*, 2011, Art. no. 79300G.
[2] M. K. Hedili, M. O. Freeman, and H. Urey, "Microlens array-based high-gain screen design for direct projection head-up displays," *Appl. Opt.*, vol. 52, no. 6, pp. 1351–1357, Feb. 2013.
[3] W. J. Horrey, C. D. Wickens, and A. L. Alexander, "The effects of head-up display clutter and in-vehicle display separation on concurrent driving performance," in *Proc. Hum. Factors Ergonom. Soc. Annu. Meeting*, 2003, pp. 1880–1884.
[4] I. Singh, A. Kumar, H. S. Singh, and O. P. Nijhawan, "Optical design and performance evaluation of a dual-beam combiner head-up display," *Opt. Eng.*, vol. 35, no. 3, pp. 813–818, Mar. 1996.
[5] Z. Qin, F. C. Lin, Y. P. Huang, and H. P. D. Shieh, "Maximal acceptable ghost images for designing a legible windshield-type vehicle head-up display," *IEEE Photon. J* ., vol. 9, no. 6, Dec. 2017, Art. no. 7000812.
[6] H. S. Park, M. W. Park, K. H. Won, K. H. Kim, and S. K. Jung, "In-vehicle AR-HUD system to provide driving-safety information," *ETRI J.*, vol. 35, no. 6, pp. 1038–1047, Dec. 2013.
[7] J. A. Betancur, J. Villa-Espinal, G. Osorio-Gómez, S. Cuéllar, and D. Suárez, "Research topics and implementation trends on automotive head-up display systems," *Int. J. Interactive Des. Manuf.*, vol. 12, no. 1, pp. 199–214, Feb. 2018.
[8] J. Zou, E. L. Hsiang, T. Zhan, K. Yin, Z. He, and S. T. Wu, "High dynamic range head-up displays," *Opt. Exp.*, vol. 28, no. 16, pp. 24298–24307, Aug. 2020.
[9] C. T. Hsieh, J. N. Shu, H. T. Chen, C. Y. Huang, C. J. Tien, and C. H. Lin, "Dual-view liquid crystal display fabricated by patterned electrodes," *Opt. Exp.*, vol. 20, no. 8, pp. 8641–8648, Apr. 2012.
[10] C. T. Hsieh *et al.*, "Twisted nematic dual-view liquid crystal display based on patterned electrodes," *J. Display Technol.*, vol. 10, no. 6, pp. 464–469, Jun. 2014.
[11] C. T. Hsieh *et al.*, "Dual-view blue phase liquid crystal display," *J. Display Technol.*, vol. 11, no. 7, pp. 575–579, Jul. 2015.
[12] J. Jeong, C. K. Lee, K. Hong, J. Yeom, and B. Lee, "Projection-type dual-view three-dimensional display system based on integral imaging," *Appl. Opt.*, vol. 53, no. 27, pp. G12–G18, Sep. 2014.
[13] Q. H. Wang, C. C. Ji, L. Li, and H. Deng, "Dual-view integral imaging 3D display by using orthogonal polarizer array and polarization switcher," *Opt. Exp.*, vol. 24, no. 1, pp. 9–16, Jan. 2016.
[14] Y. Xing, Q. H. Wang, L. Luo, H. Ren, and H. Deng, "High-performance dual-view 3-D display system based on integral imaging," *IEEE Photon. J.,* vol. 11, no. 1, Feb. 2019, Art. no. 7000212.
[15] A. Chatten *et al.*, "Systems and methods for control of vehicle functions via driver and passenger HUDs," U.S. Patent 10 562 539, Feb. 18, 2020.
[16] Y. Tokuda *et al.*, "Aerial imaging by retro-reflection with transparent retro-reflector (AIRR with TRR)," in *Proc. 22nd Int. Display Workshops*, 2014, pp. 818–819.
[17] C. Y. Shih and C. C. Tseng, "Dual-eyebox head-up display," in *Proc. 3rd IEEE Int. Conf. Intell. Transp. Eng.*, 2018, pp. 105–109.
[18] E. Moon, M. Kim, J. Roh, H. Kim, and J. Hahn, "Holographic head-mounted display with RGB light emitting diode light source," *Opt. Exp.*, vol. 22, no. 6, pp. 6526–6534, Mar. 2014.
[19] J. Zou, L. Li, and S. T. Wu, "Gaze-matched pupil steering Maxwellian-view augmented reality display with large angle diffractive liquid crystal lenses," *Adv. Photon. Res.*, vol. 3, no. 5, 2022, Art. no. 2100362.
[20] J. Han, J. Liu, X. Yao, and Y. Wang, "Portable waveguide display system with a large field of view by integrating freeform elements and volume holograms," *Opt. Exp.*, vol. 23, no. 3, pp. 3534–3549, Feb. 2015.
[21] H. Amano *et al.*, "Reconstruction of a three-dimensional color-video of a point-cloud object using the projection-type holographic display with a holographic optical element," *Opt. Exp.*, vol. 28, no. 4, pp. 5692–5705, Feb. 2020.
[22] H. Peng *et al.*, "Design and fabrication of a holographic head-up display with asymmetric field of view," *Appl. Opt.*, vol. 53, no. 29, pp. H177–H185, Oct. 2014.
[23] C. Draper, C. Bigler, M. Mann, K. Sarma, and P. Blanche, "Holographic waveguide head-up display with 2-D pupil expansion and longitudinal image magnification," *Appl. Opt.*, vol. 58, no. 5, pp. A251–A257, Feb. 2019.
[24] M. Y. He, H. L. Zhang, H. Deng, X. W. Li, D. H. Li, and Q. H. Wang, "Dual-view-zone tabletop 3D display system based on integral imaging," *Appl. Opt.*, vol. 57, no. 4, pp. 952–958, Feb. 2018.
[25] Y. Su *et al.*, "Projection-type dual-view holographic three-dimensional display and its augmented reality applications," *Opt. Commun.*, vol. 428, no. 6, pp. 216–226, Dec. 2018.
[26] H. Kogelnik, "Coupled wave theory for thick hologram gratings," *Bell Labs Tech. J.*, vol. 48, no. 9, pp. 2909–2947, Nov. 1969.
[27] J. Yeom, Y. Son, and K.-S. Choi, "Pre-compensation method for optimizing recording process of holographic optical element lenses with spherical wave reconstruction," *Opt. Exp.*, vol. 28, no. 22, pp. 33 318–33 333, Oct. 2020.
[28] Z. Lv, J. Liu, and L. Xu, "A multi-plane augmented reality head-up display system based on volume holographic optical elements with large area," *IEEE Photon. J.*, vol. 13, no. 5, Oct. 2021, Art. no. 5200108.
[29] S. Lee, B. Lee, J. Cho, C. Jang, J. Kim, and B. Lee, "Analysis and implementation of hologram lenses for see-through head-mounted display," *IEEE Photon. Technol. Lett.*, vol. 29, no. 1, pp. 82–85, Jan. 2017.
[30] C. Jang, O. Mercier, K. Bang, G. Li, Y. Zhao, and D. Lanman, "Design and fabrication of freeform holographic optical elements," *ACM Trans. Graph.*, vol. 39, no. 6, pp. 1–15, Nov. 2020.